J Mol Model (2012) 18:2343–2348
DOI 10.1007/s00894-011-1256-4

ORIGINAL PAPER

The H_2 dissociation on the BN, AlN, BP and AlP nanotubes: a comparative study

Javad Beheshtian · Hamed Soleymanabadi · Mohammad Kamfiroozi · Ali Ahmadi

Received: 28 July 2011 / Accepted: 20 September 2011 / Published online: 7 October 2011

Abstract The thermodynamic and kinetic feasibility of H_2 dissociation on the BN, AlN, BP and AlP zigzag nanotubes has been investigated theoretically by calculating the dissociation and activation energies. We determined the BN and AlP tubes to be inert toward H_2 dissociation, both thermodynamically and kinetically. The reactions are endothermic by 5.8 and 3 kcal mol^{-1}, exhibiting high activation energies of 38.8 and 30.6 kcal mol^{-1}, respectively. Our results indicated that H_2 dissociation is thermodynamically favorable on both PB and AlN nanotubes. However, in spite of the thermodynamic feasibility of H_2 dissociation on PB types, this process is kinetically unfavorable due to partly high activation energy. Generally, we concluded that among the four studied tubes, the AlN nanotube may be an appropriate model for H_2 dissociation process, from a thermodynamic and kinetic stand point. We also indicated that H_2 dissociation is not homolytic, rather it takes place via a heterolytic bond cleavage. In addition, a comparative study has been performed on the electrical and geometrical properties of the tubes. Our analysis showed that the electrical conductivity of tubes is as follows: BP>AlP>BN>AlN depending on how to combine the electron rich and electron poor atoms.

Keywords Aluminum nitride nanotubes · Aluminum phosphide nanotubes · Boron nitride nanotubes · Boron phosphide nanotubes · Density functional theory · H_2 adsorption

J. Beheshtian
Department of Chemistry,
Shahid Rajaee Teacher Training University,
P.O. Box: 16875–163, Tehran, Iran

H. Soleymanabadi
Young Researchers Club, Toyserkan Branch,
Islamic Azad University,
Toyserkan, Iran

M. Kamfiroozi
Department of Chemistry, Islamic Azad University,
Shiraz Branch,
Shiraz, Iran

A. Ahmadi (✉)
Young Researchers Club, Islamic Azad University,
Islamshahr Branch,
Tehran, Iran
e-mail: ahmadi.iau@gmail.com

Introduction

The adsorption behavior of gaseous molecules on material surfaces is a promising research subject in the development of gas sensors and catalysts. Molecular hydrogen dissociation to form atomic H species is a crucial step in numerous technologically important processes which have been investigated in great detail [1, 2]. On the other hand, hydrogen storage is one of the most important challenges for hydrogen fuel cell powered mobile applications. The conventional hydrogen storage methods such as compressed hydrogen storage system cannot meet the current and future needs. The promising development of newly discovered materials is the key to the success of hydrogen fuel cell technology.

The carbon nanotube (CNT) as a potential hydrogen storage medium has provoked enormous interests over recent years due to its light mass density and high surface to volume ratio [3]. As CNTs can be either semiconductor or metal, depending on their diameters and helicities, the experimental results reported from different groups have been controversial particularly on their capacity of hydro-

gen storage. Recently, some efforts have been made to assess inorganic nanotubes such as BN and AlN nanotubes as potential hydrogen storage mediums [4–6].

BN nanotubes are excellent inorganic nanomaterials due to their special properties such as high temperature resistance to oxygen [7], a wide band gap weakly dependent on the tube diameter, helicity, and the number of tube walls [8]. Considerably, BN nanotubes are thermally and chemically more stable than CNTs, which makes them most important in nanodevices working in hazardous and high-temperature environments [9].

To date, several studies have been published on the interaction of hydrogen atoms and molecules with BN nanotubes [10, 11]. The chemical adsorption of H atoms on a zigzag BN nanotube is studied using the density functional theory (DFT), showing that H atoms prefer to adsorb on the top sites of adjacent B and N atoms to form an armchair chain along the tube axis [12].

Zhang et al. predicted that AlN nanotubes are energetically favorable and arrange in a hexagonal network adopting an sp^2 hybridization for both N and Al atoms [13]. Tondare et al. successfully synthesized the AlNNTs with diameter ranging from 30–80 nm [14]. Recently, the other papers have been reported on the synthesis of AlNNTs through different methods [15, 16]. Recently, Lim and Lin have reported an ab initio study of the hydrogen chemisorption on single-walled AlN nanotubes, showing that the calculated energy barrier and the energy of reaction is about 0.89 and - 0.11 eV, respectively [4]. In addition, we have shown that the NH_3 adsorption capacity of AlN nanotubes is typically more than that of BN types [17, 18].

Several studies have been focused on the other inorganic nanotubes including: PB and AlP nanotubes [19–21]. Baei et al. have studied the behavior of H_2O_2 adsorbed inside a BP nanotube investigating the nature of this interaction [22]. They have shown that the binding energies and the dipole moments of the nanotube depend on the orientation and location of the H_2O_2 inside the tube. Mirzaei et al. have explored electronic structures and NMR parameters of pristine and several doped types of both BP and AlP nanotubes [23–25].

Here, we are interested in a comparative theoretical study on the H_2 dissociation on BN, AlN, BP and AlP nanotubes. We also comparatively will investigate their structural and electrical properties under identical conditions. We believe that our study can help researchers working on development of gas sensors, filters, electro-nanodevices and H_2 storage materials.

Computational details

We selected four finite-length zigzag (5,0) nanotubes including: BN, AlN, BP and AlP types, Fig. 1. The atoms at the open ends of the tubes were saturated by hydrogen atoms to avoid the boundary effects. Generally, the molecular formula of these tubes are $X_{27}Y_{27}H_{10}$; X=B, Al and Y=N, P. Structure optimizations and transition state (TS) calculations were obtained at uB3LYP/3-21G* level of theory while natural bond orbital (NBO), density of states (DOS), molecular electrostatic potential (MEP) analyses and all energy calculations were performed using uB3LYP/6-31G** level . We define the dissociation energy (E_{dis}) of H_2 as follows

$$E_{dis}=E_{tot}(H-tube-H)-E_{tot}(tube)-E_{tot}(H_2),$$

where E_{tot}(H-tube-H) is the total energy of a tube after dissociation of an H_2 molecule on its surface, and the E_{tot}(tube) or $E_{tot}(H_2)$ are the total energies of a bare tube or an isolated single H_2 molecule. A negative or positive value of E_{dis} is referred to as an exothermic or endothermic process.

The B3LYP/6-31G* is the commonly used level of theory in investigations of nanotube systems [23–28]. However, we improved it by adding the polarization p-function to basis sets of hydrogen atoms (the second star) to get a high-quality description of H_2 dissociation process. Harmonic vibrational frequency calculations confirmed the stationary point as a TS structure with one imaginary frequency whose normal mode corresponds with the reaction coordinate. All calculations reported here were carried out using a locally modified version of the GAMESS electronic structure program [29].

Results and discussion

At first, the accuracy of the method used in this work has been tested initially to describe the properties of H_2 molecule in gas phase. The bond length and vibrational frequency of molecular H_2 calculated from our approach are 0.746 Å and 4416.8 cm^{-1}, which are in good consistency with the experimental values of 0.740 Å [30] and 4401 cm^{-1} [31], respectively.

The optimized structures of the studied nanotubes with the geometrical parameters for selected X and Y atoms are summarized in Fig. 1. The results indicate that the equilibrium bond length of X-Y for BN, AlN, BP and AlP nanotubes are 1.48, 1.82, 189 and 2.29 Å, respectively. The small size of angles around the P atoms is related to their hybridization. As shown in Table 1, based on the NBO analysis the hybridization of electron rich P and N atoms is nearly sp^3 and sp^2, respectively, while that is sp^2 for both electron poor B and Al atoms. Diameters and length of the optimized BN, AlN, BP and AlP tubes are shown in Table 2. Diameter is defined as the maximum distance of two atoms in one layer of tube center.

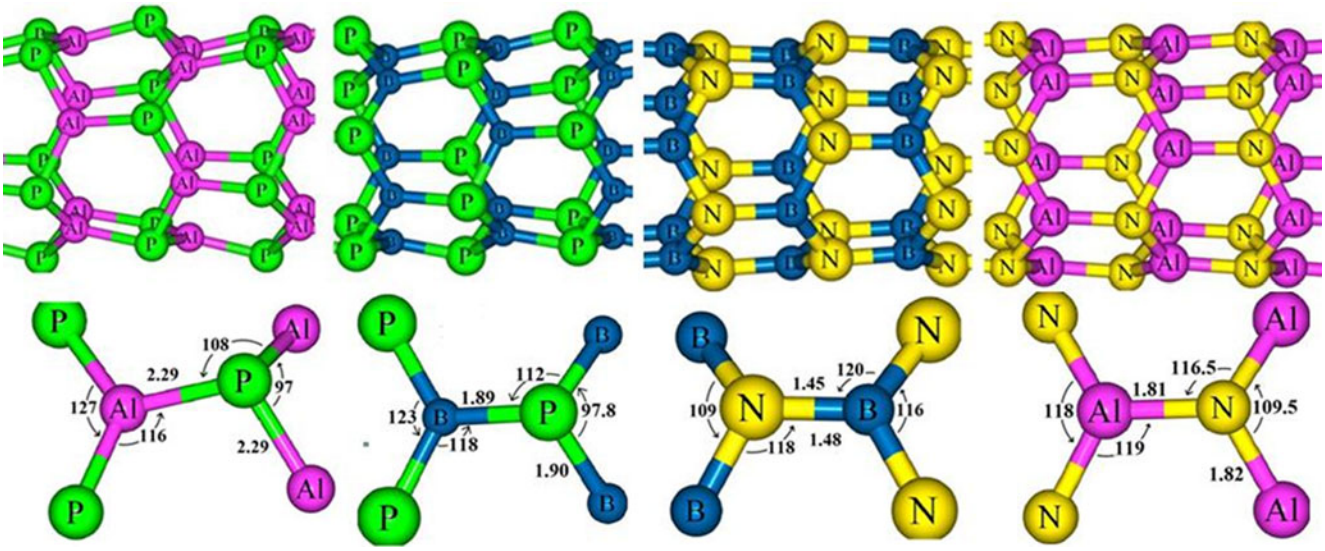

Fig. 1 The optimized structures and geometry parameters of BN, AlN, AlP and BP nanotubes

It is clear that the larger size of diameter and length is related to the larger size of forming atoms. For example, AlP tube has the largest diameter and length due to the large covalent radius of P and Al atoms. The Mulliken charges are transferred from the electropositive atom (X) to the electronegative one (Y) in surfaces of BN, AlN, BP and AlP tubes are 0.54, 0.82, 0.13 and 0.25 electrons, respectively (Table 2). Our calculations show that there is a linear relation between the charge transferred and the electronegativity difference between the X and Y atoms with R-square value of 0.906 (Fig. 2). However, the ionicity of the Al-N and B-N bonds is significantly more than that of both B-P and Al-P types.

Our HOMO/LUMO energy gap (E_g) analysis (Table 2) show that the magnitudes of E_g (in eV) for the studied tubes are as follows:

$$\mathrm{AlN}(4.11) > \mathrm{BN}(3.37) > \mathrm{AlP}(2.62) > \mathrm{BP}(1.62).$$

The BP nanotube has the smallest E_g among all types; therefore, it is the most electrically conductive nanotube. The AlN case has the most electrical resistivity due to the largest E_g. It seems that there is a definite relation between the size of consisting atoms and E_g of tubes, *i.e.*, the tubes that consist of the larger electron rich and smaller electron poor atoms has smaller E_g. It can be rationalized by this fact that the HOMOs of tubes are localized on the electron rich atoms (P and N) with high polarizability and the LUMOs on the electron poor ones. It is apparent that the lone pairs of P atoms can easily be transferred to the LUMO of B or Al atom, in comparison to those of N ones, justifying the small E_g of P involved tubes compared with that of N involved ones.

Here, we focused on the H_2 dissociation on X-Y bond, parallel with tube axis. Firstly, we assumed that a H_2 molecule moving toward the tube surface is broken into two H atoms, forming two new bonds including: X-H and Y-H. The TS and final structures with geometrical parameters are shown in Fig. 3. Secondly, we probed the thermodynamic and kinetic possibility of these processes, assessing the energies of activation barrier and reaction.

The calculated E_{dis} values (Table 2) are positive for BN and AlP tubes about 5.8 and 3.0 kcal mol^{-1}, indicating that this process is thermodynamically unfavorable. In addition, the calculated activation energies are large about 38.8 and 30.6 kcal mol^{-1}, respectively. A hydrogen molecule, however, prefers to dissociate on both AlN and BP tube surface, with adsorption energies of −9.1 and −13.4 kcal mol^{-1}, respectively. These processes are energetically favorable and

Table 1 The hybridization of X (electropositive atom) and Y (electronegative atom) in surfaces of nanotubes obtained from NBO analysis

Y	X	Tube
$sp^{1.86}$	$sp^{2.1}$	BN
$sp^{2.03}$	$sp^{1.99}$	AlN
$sp^{3.22}$	$sp^{1.96}$	BP
$sp^{3.91}$	$sp^{2.04}$	AlP

Table 2 The calculated diameter (Å), length (Å), HOMO/LUMO energy gap (E_g), and Mulliken charge transfer from Y to X atom of tube surfaces plus the energies (kcal mol^{-1}) of H_2 dissociation (E_{dis}) and activation (E_{act})on the BN, AlN, BP and AlP nanotubes

Tube	Diameter	Length	E_g(eV)	Q_T (e)	E_{act}	E_{dis}
BN	4.26	11.56	3.37	0.54	38.8	2.60
AlN	5.25	14.06	4.11	0.82	18.0	1.96
BP	5.39	14.64	1.62	0.13	30.6	2.60
AlP	6.63	17.34	2.62	0.25	27.3	1.74

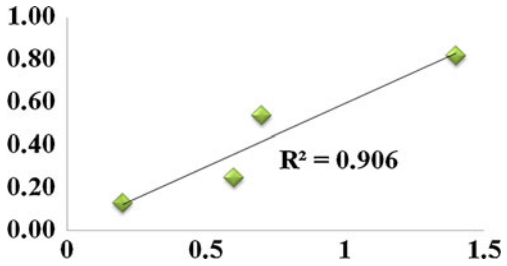

Fig. 2 The linear relation between the charge transferred (the vertical vector) and the electronegativity difference between the X and Y (the horizontal vector)

exothermic. The activation barrier is rather low (18 kcal mol^{-1}; 0.78 eV) for AlN case, indicating that chemisorption is a feasible route for hydrogen storage in this type of nanotube. The calculated activation energy for AlN tube is essentially the same as the value obtained in earlier theoretical study by Li et al. on AlN nanowires, about 0.76 eV [32]. Despite the thermodynamic feasibility of H_2 dissociation on PB types, this process is kinetically unfavorable due to partly high activation energy about 27.3 kcal mol^{-1}. Among the all studied tubes, one can conclude that AlN nanotubes may be the most appropriate for H_2 dissociation from a thermodynamic and kinetic stand point. In Fig. 4, we have sketched energy levels

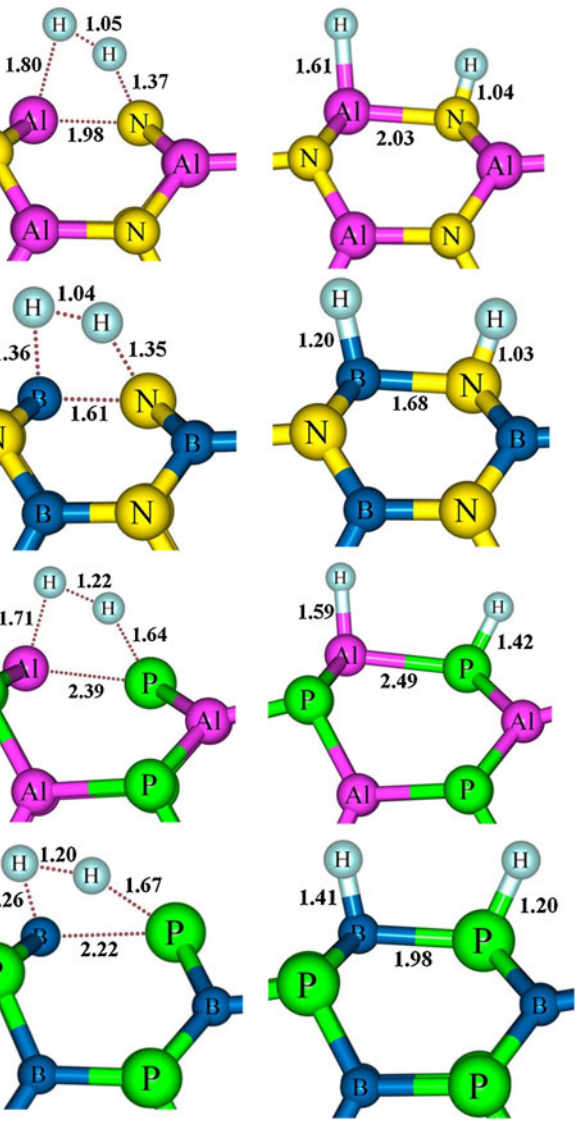

Fig. 3 The optimized geometrical parameters of transition states (left hand) and final structures (right hand) of H_2 dissociation on AlN, BN, AlP and BP nanotubes. The bondlengths are in angstrom

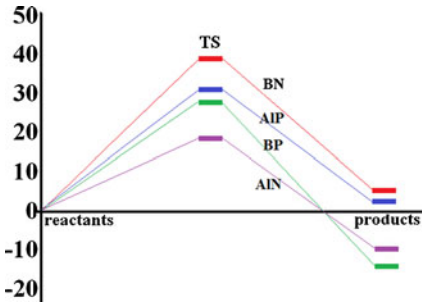

Fig. 4 The energy diagram for H_2 dissociation on the different nanotubes including: BN, AlP, BP and AlN. The energy is in kcal mol^{-1}. The energies of reactants have been taken as the reference point with energy equal to zero

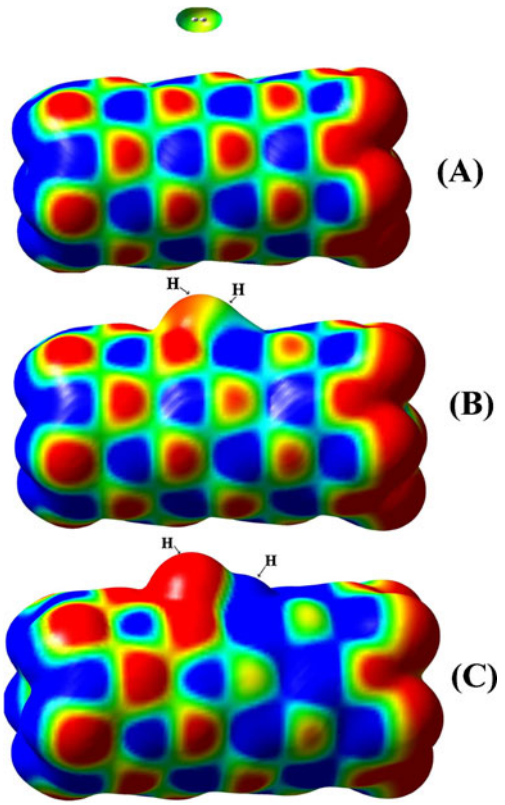

Fig. 5 The molecular electrostatic surfaces (MEP) for (**a**) H_2 molecule and AlN nanotube far enough apart from each other (**b**) transition state (TS) (**c**) final state. Color range, in a.u.: - 0.02 (red), + 0.02 (blue)

of the substrate, TS and product for each reaction. The energies of reactants have been taken as the reference point with energy equal to zero.

However, as shown in Table 2 and Fig. 4 , the thermodynamic feasibility of H_2 dissociation on mentioned nanotube surfaces are in order of BP>AlN>AlP>BN; the observed trend is related to the energy of breaking or weakening and forming new bonds during the dissociation process. For example in the case of BP the bond length of B-P (the bond that H_2 dissociates on it) is about 1.89 and 1.98 Å before and after H_2 dissociation, respectively, showing a small change of 0.09 Å (about 4.8%). However this change for the case of BN (as thermodynamically the most unfavorable system toward this process) is about 13.5 %. We note that to gain a general conclusion one must consider energies of all breaking and forming bonds, here we mentioned only an example.

Here, we interpret the mechanism of H_2 dissociation on X-Y bond of tubes. To this end, we calculated the MEP surfaces for the AlN nanotube and its H_2 adsorbed transition and final state as a representative model. We selected the AlN tube due to its thermodynamic and kinetic possibility toward this process. The MEP at an atomic site can be defined as follows:

$$V(r) = \sum_A \frac{Z_A}{|R_A - r|} - \int \frac{\rho(r')dr'}{|r' - r|}, \quad (1)$$

where Z_A is the charge on nucleus A, located at R_A. The sign of V(r) depends on whether the effects of the nuclei or the electrons are dominant at any point. The MEP has frequently been used to explore the chemical properties [33–36].

As shown in Fig. 5a, when the H_2 molecule and AlN nanotube are far enough apart from each other there is no overlap between their electron densities. Surface of AlN nanotube shows characteristic patterns of alternating positive and negative regions and the identical color of the entire surface of H_2 confirms its non-polar bond. As shown in panel B of Fig. 5, when H_2 molecule approaches the tube surface (TS configuration) the heteropolar nature of Al-N bond of tube induces a dipole on it, such that one of the H atoms which is closer to the Al atom has more electron density (light red color in the figure).

In the final state (Fig. 5c) H_2 completely dissociates into two H atom (or ions), locating the colors of blue or red on them. It indicates that this process is not homolytic dissociation but take places via a heterolytic bond cleavage. It can be rationalized scrutinizing the MEP of final state which in blue color (positive charge) is completely located around the newly formed N-H bond, indicating that an H^+ is transferred to this site.

It is noteworthy to say that the heterolytic H_2 bond cleavage requires energy to completely separate the negative and positive charges over H-H bond. It seems that the electronegativity difference between the atoms in the different tubes can help this process through inducing a polarization on the H-H bond. In addition, the energy required for heterolityc bond cleavage may be reduced below that for homolytic cleavage in the presence of polar substrates that stabilize the ions produced.

A similar trend is observed for newly formed Al-H bond, *i.e.*, a red color (negative charge) is completely located around the newly formed N-H bond, indicating that an electron rich H is transferred to this site. In TS the empty antibonding $1\sigma_u$* orbital of H_2 becomes partially occupied, weakening the H-H bond slightly. This phenomenon can help the shift of H with pair electrons of $1\sigma_g$ orbital to the empty orbital of Al atom.

Finally, chemical dative Al-H and N-H bonds with the surface start to form, with Wiberg bond indexes (WBI) [37] of 0.75 and 0.76, respectively. The WBIs of X-H and Y-H covalent bonds ends of tube are slightly higher with values of 0.80 and 0.81, respectively.

Conclusions

We theoretically explored the thermodynamic and kinetic feasibility of H_2 dissociation on BN, AlN, BP and AlP nanotubes by calculating dissociation and activation energies. Our B3LYP calculations reveal that this process is thermodynamically favorable on PB and AlN nanotubes. Despite the thermodynamic feasibility of H_2 dissociation on PB types, this process is kinetically unfavorable because of the relatively high activation energy, 27.3 kcal mol^{-1}. It was found that the BN and AlP tubes are inert toward H_2 dissociation, both thermodynamically and kinetically. The reactions are endothermic by 5.8 and 3.0 kcal mol^{-1}, exhibiting high activation energies of 38.8 and 30.6 kcal mol^{-1}, respectively. Finally, we concluded that among the four studied tubes, the AlN nanotube may be an appropriate model for H_2 dissociation process from a thermodynamic and kinetic stand point, with dissociation and activation energy of −9.1 and 18 kcal mol^{-1}. Additionally, we performed a comparative study on the electrical and geometrical properties of the tubes, indicating that the electrical conductivity of tubes is as follows: BP>AlP>B-N>AlN depending on the electron rich and electron poor atoms are combined.

References

1. Zhang R, Ling L, Wang B (2010) Theoretical studies on reaction mechanism of H_2 with COS. J Mol Model 16:1911–1917. doi:10.1007/s00894-010-0686-8

2. Zhou C, Yao S, Zhang Q, Wu J, Yang M, Forrey R, Cheng H (2011) Hydrogen sequential dissociative chemisorption on Ni(n) (n=2 9,13) clusters: comparison with Pt and Pd. J Mol Model 1–7. doi:10.1007/s00894-011-1059-7
3. Knippenberg M, Stuart S, Cheng H (2008) Molecular dynamics simulations on hydrogen adsorption in finite single walled carbon nanotube bundles. J Mol Model 14:343–351. doi:10.1007/s00894-008-0275-2
4. Lim SH, Lin J (2008) Ab initio study of the hydrogen chemisorption of single-walled aluminum nitride nanotubes. Chem Phys Lett 466:197–204
5. Han SS, Lee SH, Kang JK, Lee HM (2005) High coverage of hydrogen on a (10,0) single-walled boron nitride nanotube. Phys Rev B 72:113402
6. Cheng J, Ding R, Liu Y, Ding Z, Zhang L (2007) Computer simulation of hydrogen physisorption in single-walled boron nitride nanotube arrays. Comput Mater Sci 40:341–344
7. Golberg D, Bando Y, Eremets M, Takemura K, Kurashima K, Yusa H (1996) Nanotubes in boron nitride laser heated at high pressure. Appl Phys Lett 69:2045–2047
8. Rubio A, Corkill JL, Cohen ML (1994) Theory of graphitic boron nitride nanotubes. Phys Rev B 49:5081–5084
9. Hern, aacute, ndez E, Goze C, Bernier P, Rubio A (1998) Elastic properties of C and BxCyNz composite nanotubes. Phys Rev Lett 80:4502–4505
10. Jhi S-H, Kwon Y-K (2004) Hydrogen adsorption on boron nitride nanotubes: a path to room-temperature hydrogen storage. Phys Rev B 69:245407–2454010
11. Wu X, Yang JL, Zeng XC (2006) Adsorption of hydrogen molecules on the platinum-doped boron nitride nanotubes. J Chem Phys 125:44704–44709
12. Wu X, Yang J, Hou JG, Zhu Q (2004) Hydrogen adsorption on zigzag (8,0) boron nitride nanotubes. J Chem Phys 121:8481–8485
13. Zhang D, Zhang RQ (2003) Theoretical prediction on aluminum nitride nanotubes. Chem Phys Lett 371:426–432. doi:10.1016/s0009-2614(03)00289-6
14. Tondare VN, Balasubramanian C, Shende SV, Joag DS, Godbole VP, Bhoraskar SV, Bhadbhade M (2002) Field emission from open ended aluminum nitride nanotubes. Appl Phys Lett 80:4813–4815
15. Balasubramanian C, Bellucci S, Castrucci P, De Crescenzi M, Bhoraskar SV (2004) Scanning tunneling microscopy observation of coiled aluminum nitride nanotubes. Chem Phys Lett 383:188–191. doi:10.1016/j.cplett.2003.11.028
16. Stan G, Ciobanu CV, Thayer TP, Wang GT, Creighton JR, Purushotham KP, Bendersky LA, Cook RF (2009) Elastic moduli of faceted aluminum nitride nanotubes measured by contact resonance atomic force microscopy. Nanotechnology 20:35706–357014
17. Ahmadi A, Beheshtian J, Hadipour NL (2011) Interaction of NH_3 with aluminum nitride nanotube: electrostatic vs. covalent. Physica E 43:1717–1719
18. Ahmadi A, Kamfiroozi M, Beheshtian J, Hadipour N. The effect of surface curvature of aluminum nitride nanotubes on the adsorption of NH_3. Struct Chem. doi:10.1007/s11224-011-9820-1
19. Mirzaei M, Mirzaei M (2011) A theoretical study of boron-doped aluminum phosphide nanotubes. Comput Theor Chem 963:294–297
20. Mirzaei M (2011) Carbon doped boron phosphide nanotubes: a computational study. J Mol Mod 17:89–96. doi:10.1007/s00894-010-0702-z
21. Baei M, Sayyad-Alangi S, Moradi A, Torabi P (2011) NMR and NQR parameters of the SiC-doped on the (4,4) armchair single-walled BPNT: a computational study. J Mol Model. doi:10.1007/s00894-011-1130-4
22. Baei M, Moradi A, Torabi P, Moghimi M (2011) Adsorption properties of H_2O_2 trapped inside a boron phosphide nanotube. Monatshefte für Chemie / Chemical Monthly:1–5. doi:10.1007/s00706-011-0548-9
23. Mirzaei M, Mirzaei M (2010) Aluminum phosphide nanotubes: density functional calculations of aluminum-27 and phosphorus-31 chemical shielding parameters. Theochem 951:69–71
24. Mirzaei M, Mirzaei M (2011) The C-doped AlP nanotubes: a computational study. Solid State Sci 13:244–250
25. Mirzaei M, Giahi M (2010) Computational studies on boron nitride and boron phosphide nanotubes: density functional calculations of boron-11 electric field gradient tensors. Physica E 42:1667–1669
26. Ruangpornvisuti V (2010) Molecular modeling of dissociative and non-dissociative chemisorption of nitrosamine on close-ended and open-ended pristine and Stone-Wales defective (5,5) armchair single-walled carbon nanotubes. J Mol Model 16:1127–1138. doi:10.1007/s00894-009-0622-y
27. Ahmadi A, Beheshtian J, Kamfiroozi M, Benchmarking of ONIOM method for the study of NH_3 dissociation at open ends of BNNTs. J Mol Model. doi:10.1007/s00894-011-1202-5
28. Ahmadi A, Beheshtian J, Hadipour N (2011) Chemisorption of NH_3 at the open ends of boron nitride nanotubes: a DFT study. Struct Chem 22:183–188. doi:10.1007/s11224-010-9697-4
29. Schmidt MW, Baldridge KK, Boatz JA, Elbert ST, Gordon MS, Jensen JH, Koseki S, Matsunaga N, Nguyen KA, Su S, Windus TL, Dupuis M, Montgomery JA (1993) General atomic and molecular electronic structure system. J Comput Chem 14:1347–1363. doi:10.1002/jcc.540141112
30. Wu G, Zhang J, Wu Y, Li Q, Chou K, Bao X (2009) Adsorption and dissociation of hydrogen on MgO surface: a first-principles study. J Alloy Comp 480:788–793. doi:10.1016/j.jallcom.2009.02.086
31. Huber K, Herzberg G (1979) Molecular spectra, molecular structure: constants vol. IV. Reinhold, New York
32. Yafei L et al (2009) Computational studies on hydrogen storage in aluminum nitride nanowires/tubes. Nanotechnology 20:215701–215708
33. Politzer P, Murray J, Lane P, Concha M, Jin P, Peralta-Inga Z (2005) An unusual feature of end-substituted model carbon (6,0) nanotubes. J Mol Model 11:258–264. doi:10.1007/s00894-005-0265-6
34. Murray JS, Abu-Awwad F, Politzer P (2000) Characterization of aromatic hydrocarbons by means of average local ionization energies on their molecular surfaces. Theochem 501–502:241–250. doi:10.1016/s0166-1280(99)00435-2
35. Sjoberg P, Politzer P (1990) Use of the electrostatic potential at the molecular surface to interpret and predict nucleophilic processes. J Phys Chem 94:3959–3961. doi:10.1021/j100373a017
36. Gross KC, Seybold PG, Peralta-Inga Z, Murray JS, Politzer P (2001) Comparison of quantum chemical parameters and hammett constants in correlating pKa values of substituted anilines. J Org Chem 66:6919–6925. doi:10.1021/jo010234g
37. Wiberg KB (1968) Application of the pople-santry-segal CNDO method to the cyclopropylcarbinyl and cyclobutyl cation and to bicyclobutane. Tetrahedron 24:1083–1096